PLOS ONE

RESEARCH ARTICLE

Tumor Repression of VCaP Xenografts by a Pyrrole-Imidazole Polyamide

Amanda E. Hargrove[1¤a], Thomas F. Martinez[1], Alissa A. Hare[1¤b], Alexis A. Kurmis[1], John W. Phillips[1¤c], Sudha Sud[2], Kenneth J Pienta[2¤d]*, Peter B. Dervan[1]*

1 Division of Chemistry and Chemical Engineering, California Institute of Technology, Pasadena, California, United States of America, **2** Department of Urology, University of Michigan Medical School, Ann Arbor, Michigan, United States of America

¤a Current address: Department of Chemistry, Duke University, Durham, North Carolina, United States of America
¤b Current address: Department of Chemistry, Vanderbilt University, Nashville, Tennessee, United States of America
¤c Current address: Department of Microbiology, Immunology and Medical Genetics, University of California Los Angeles, Los Angeles, California, United States of America
¤d Current address: Departments of Urology and Oncology, and Brady Urological Institute, The Johns Hopkins Medical Institutions, Baltimore, Maryland, United States of America
* dervan@caltech.edu (PBD); kpienta1@jhmi.edu (KJP)

Citation: Hargrove AE, Martinez TF, Hare AA, Kurmis AA, Phillips JW, Sud S, et al. (2015) Tumor Repression of VCaP Xenografts by a Pyrrole-Imidazole Polyamide. PLoS ONE 10(11): e0143161. doi:10.1371/journal.pone.0143161

Editor: Irina U Agoulnik, Florida International University, UNITED STATES

Received: July 21, 2015

Accepted: November 2, 2015

Published: November 16, 2015

Data Availability Statement: All relevant data are within the paper and its Supporting Information files.

Funding: The research has been supported by the National Institutes of Health (www.nih.gov, Grants R01GM027681 to PBD, F32CA156833 to AEH, F31CA159896 to TFM, F32CA173977 to AAH, and T32GM007616 to AAK) and the Prostate Cancer Foundation (www.pcf.org). The funders had no role in study design, data collection and analysis, decision to publish, or preparation of the manuscript.

Competing Interests: The authors have declared that no competing interests exist.

Abstract

Pyrrole-imidazole (Py-Im) polyamides are high affinity DNA-binding small molecules that can inhibit protein-DNA interactions. In VCaP cells, a human prostate cancer cell line over-expressing both AR and the *TMPRSS2-ERG* gene fusion, an androgen response element (ARE)-targeted Py-Im polyamide significantly downregulates AR driven gene expression. Polyamide exposure to VCaP cells reduced proliferation without causing DNA damage. Py-Im polyamide treatment also reduced tumor growth in a VCaP mouse xenograft model. In addition to the effects on AR regulated transcription, RNA-seq analysis revealed inhibition of topoisomerase-DNA binding as a potential mechanism that contributes to the antitumor effects of polyamides in cell culture and in xenografts. These studies support the therapeutic potential of Py-Im polyamides to target multiple aspects of transcriptional regulation in prostate cancers without genotoxic stress.

Introduction

Pyrrole imidazole (Py-Im) polyamides are non-covalent, sequence specific DNA binders that can alter DNA architecture [1, 2]. Upon high affinity binding to the DNA minor groove, the molecules cause a 4 angstrom widening of the minor groove walls and a corresponding compression of the opposing major groove [3, 4]. Despite the relatively large molecular weight of Py-Im polyamides, these molecules are cell permeable and localize to the cell nucleus to affect endogenous gene expression [5–10]. Due to their modular sequence specificity, Py-Im polyamides can be synthesized to target DNA sequences of similar size to a protein-DNA interaction site and therefore used to antagonize gene expression driven by specific transcription factors [7, 9–13]. One such transcription factor that has been studied previously is the androgen receptor (AR) [9].

The AR is a dihydrotestosterone (DHT) inducible nuclear hormone receptor whose transcriptional program has been implicated in the progression of prostate cancer [14–16]. Upon ligand induction, AR will homodimerize, translocate to the nucleus and bind to conserved sequences known as the androgen response element (ARE) to regulate transcription [17]. Each monomeric unit binds to a half site of the sequence 5'-TGTTCT-3' [18]. Polyamide **1** (Fig 1) was designed to target the sequence 5'-WGWWCW-3' (W = A/T), found in a subset of ARE half-sites, and has been shown to prevent AR binding at select AREs and attenuate AR signaling [9].

In addition to antagonizing AR signaling, polyamide **1** is also cytotoxic towards prostate cancer cells [19]. Experiments in mice have shown that polyamide **1** is bioavailable via several routes of administration, with a serum half-life of 5.2 hours [20, 21]. In xenograft experiments, polyamide **1** has been shown to be active towards LNCaP xenografts at doses of 1 mg/kg [19]. LNCaP, however, expresses a mutated androgen receptor, and as a result, may not be representative of the majority of human disease [22]. It would therefore be useful to evaluate the efficacy of **1** against other forms of prostate cancer.

The VCaP human prostate cancer cell line expresses wild type AR and contains the *TMPRSS2-ERG* fusion [23]. Gene fusions between the *TMPRSS2* 5'-untranslated region and the *ERG* oncogene are found in approximately half of prostate cancer cases [24]. The fusion allows the AR regulated *TMPRSS2* promoter to drive the expression of *ERG*, and overexpression of *ERG* in patients has been linked with higher incidences of metastasis and poor disease prognosis [25]. In cell culture, *ERG* overexpression in immortalized prostate RPWE epithelial cells and in primary prostate epithelial cells (PrEC) has been shown to increase cellular invasiveness [26]. Due to these characteristics, the VCaP cell line presents an ideal model for the study of Py-Im polyamide activity towards this common subtype of prostate cancer. In this study, we evaluated the activity of the ARE targeted polyamide **1** in VCaP cells.

Materials and Methods

Synthesis and quantitation of Py-Im polyamide 1

Chemicals were obtained from Sigma Aldrich or Fisher Scientific unless otherwise noted. Synthesis was performed using previously reported procedures as indicated [7, 27]. Briefly, polyamides were synthesized by microwave-assisted solid phase synthesis on Kaiser oxime resin (Nova Biochem) [27] and then cleaved from the resin with neat 3,3'-diamino-*N*-methyldipropylamine. The triamine-conjugated polyamides were purified by reverse phase HPLC and subsequently modified at the C-terminus with isophthalic acid (IPA) or fluorescein-5-isothiocyanate (FITC isomer I, Invitrogen) [7]. The amine substituents of the γ-aminobutyric acid (GABA) turn units of the polyamides were deprotected using neat trifluoroacetic acid [28, 29]. The final polyamide was purified by reverse phase HPLC, lyophilized to dryness, and stored at -20°C. The identity and purity of the final compounds were confirmed by matrix-assisted laser desorption/ionization time-of-flight (MALDI-TOF) spectrometry and analytical HPLC. Chemical structures are represented in Fig 1 and S1 Fig Mass spectrometry characterization data are represented in S2 Fig.

Py-Im polyamides were dissolved in sterile dimethylsulfoxide (DMSO, ATCC) and quantitated by UV spectroscopy in either 4:1 0.1% TFA (aqueous):acetonitrile (ε(310nm) = 69,500 $M^{-1}cm^{-1}$) or 9:1 water:DMSO (ε(310nm) = 107,100 $M^{-1}cm^{-1}$) as dictated by solubility. Polyamides were added to cell culture solutions at 1000x concentration to give 0.1% DMSO solutions.

Cell culture

The VCaP cell line was obtained from the laboratories of Dr. Kenneth J. Pienta and Dr. Arul M. Chinnaiyan at the University of Michigan Department of Pathology, where the cell line was

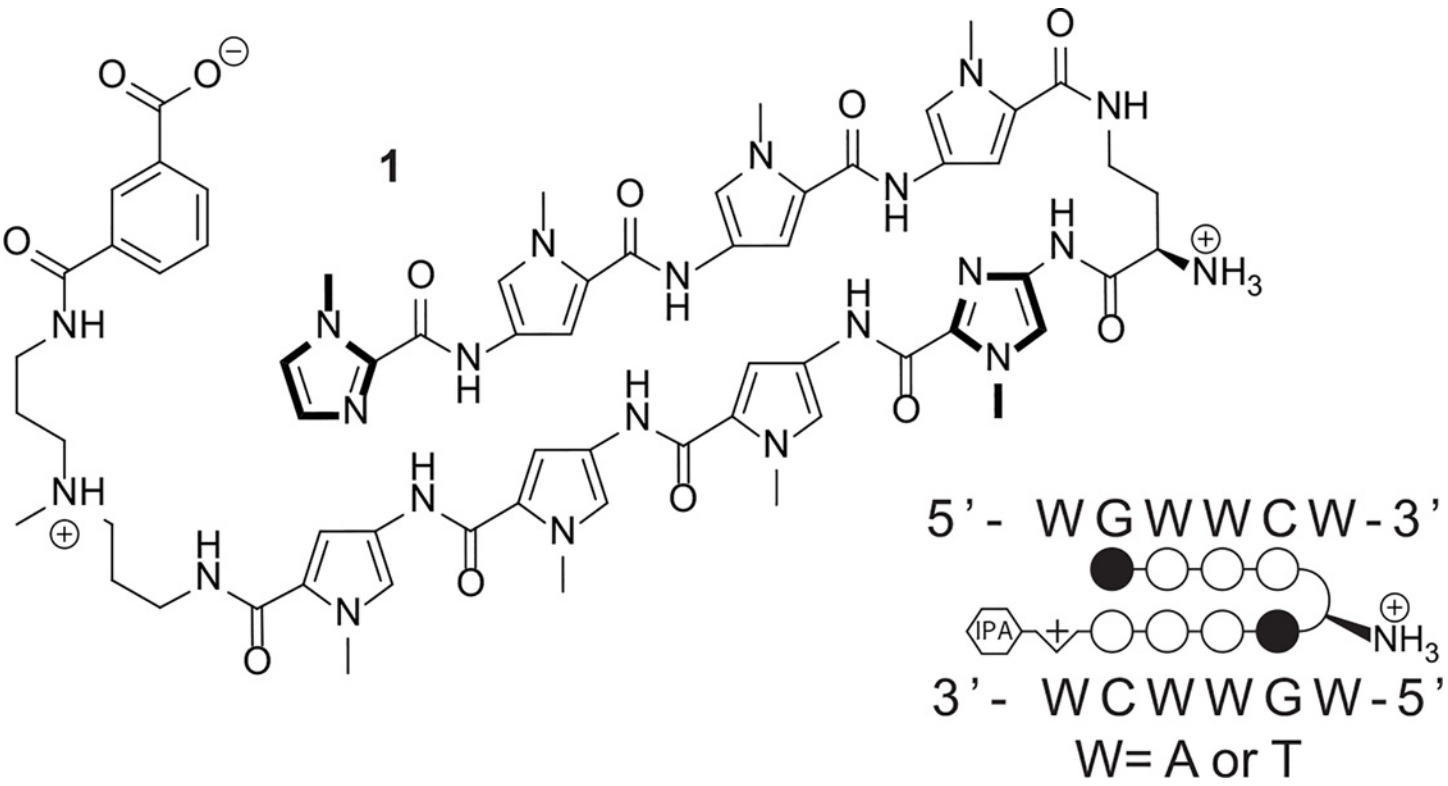

Fig 1. Chemical structure of a Py-Im polyamide (1) designed to target the DNA sequence 5′-WGWWCW-3′. A ball and stick notation is used to represent binding to the target DNA sequence. Pairing of an imidazole heterocycle (black circle) with a pyrrole heterocycle (white circle) allows G•C recognition, and the pairing of two pyrrole heterocycles recognizes A•T or T•A base pairs.

doi:10.1371/journal.pone.0143161.g001

derived [30]. VCaP cells were received at passage 19 and cultured in Dulbecco's modified eagle medium (DMEM, Gibco 10313–039) with 4 mM glutamine (Invitrogen) and fetal bovine serum (FBS, Omega Scientific) on Corning CellBind flasks. All experiments were performed below passage 30.

Cellular uptake studies

For visualization of uptake using FITC-analog polyamides, VCaP cells were plated in 35-mm optical dishes (MatTek) at 7.5×10^4 cells per dish and allowed to adhere for 48 h. Media was then changed and cells were treated with 0.1% DMSO with polyamide for 24 or 48 h. Cells were imaged at the Caltech Beckman Imaging Center using a Zeiss LSM 5 Exciter inverted laser scanning microscope equipped with a 63x oil immersion lens as previously described [5].

WST-1 proliferation assay

VCaP cells were plated at $2x10^4$ per well in 96-well plates coated with poly-L-lysine (BD Bio-Coat). After 24 h, an additional volume of medium containing vehicle or polyamide was added to each well. All medium was removed following polyamide incubation at the indicated time points and replaced with one volume of WST-1 reagent (Roche) in medium according to manufacturer protocol. After 4 h of incubation at 37°C, the absorbance was measured on a FlexStation3 plate reader (Molecule Devices). The value of A(450 nm)-A(630 nm) of treated cells was referenced to vehicle treated cells. Non-linear regression analysis (Prism software, Graphpad) was performed to determine IC_{50} values.

Gene expression analysis by quantitative RT-PCR (qPCR)

For DHT induction experiments, VCaP cells were plated in 6-well plates coated with poly-L-lysine (BD BioCoat) in charcoal-treated FBS containing media at a density of 31k/cm^2 (3x10^5 cells per well). The cells were allowed to adhere for 24 h and then dosed with 0.1% DMSO with or without polyamide **1** for 72 h followed by the addition of 0.01% ethanol in PBS with or without DHT (1 nM final concentration). Cells were harvested after additional 24 h incubation. Cells treated with etoposide and camptothecin (Sigma) were co-treated with DHT (1 nM) and harvested after a 16 h incubation. For native expression experiments, VCaP cells were plated as above but using standard FBS media and harvested after 72 h of treatment. For all experiments, the mRNA was extracted using the QIAGEN® RNeasy mini kit following the standard purification protocol. Samples were submitted to DNAse treatment using the TURBO DNA-*free*™ Kit (Ambion), and the mRNA was reverse-transcribed by using the Transcriptor First Strand cDNA Synthesis Kit (Roche). Quantitative PCR was performed by using the FastStart Universal SYBR Green Master (Rox) (Roche) on an ABI 7300 Real Time PCR System. Gene expression was normalized against *GUSB*. Primers used are referenced in S3 Fig.

Immunoblot of ERG protein levels

For assessment of ERG and beta-actin protein levels, 3x10^6 VCaP cells were plated in 10 cm diameter dishes with charcoal-treated FBS containing media for 24 h before treatment with 0.1% DMSO vehicle with or without polyamide **1** for an additional 72 h. Ethanol (0.01%) in PBS with or without DHT (1 nM final concentration) was then added. After 24 h incubation, cells were lysed in TBS-Tx buffer (50 mM Tris-HCl pH 7.4, 150 mM NaCl, 1 mM EDTA, 1% Triton X100) containing fresh 1 mM phenylmethanesulfonylfluoride (PMSF) and protease inhibitors (Roche). The samples were quantified by Bradford assay, denatured by boiling in Laemmli buffer, and total protein was separated by SDS-PAGE. After transfer to the polyvinyl difluoride (PVDF) membrane (Bio-Rad) and blocking with Odyssey Blocking Buffer (LI-COR), primary antibodies were incubated overnight at 4°C. Rabbit monoclonal anti-ERG antibody (Epitomics 2805–1) and rabbit polyclonal anti-actin antibody (Sigma A2066) were used. Goat anti-rabbit near-IR conjugated secondary antibody (LI-COR) was added and the bands were visualized on an Odyssey infrared imager (LI-COR). The experiment was conducted in duplicate and the data are representative of both trials.

Single cell electrophoresis (COMET) assay

VCaP cells (3x10^6 cells) were plated in 10 cm cell culture dishes and allowed to adhere for 24 h before addition of DMSO vehicle or polyamide stock in DMSO. After 72 h incubation, cells were washed with warm PBS (37°C), gently scraped, and counted. Samples were centrifuged, resuspended at 1x10^5 cells/mL, and treated according to manufacturer protocol (Trevigen) for neutral electrophoresis. Slides were stained with SybrGreen (Trevigen) and imaged at the Caltech Beckman Imaging Center using a Zeiss LSM 5 Pascal inverted laser scanning microscope equipped with a 5x air objective lens. Overlayed fluorescence and bright field images were obtained using standard filter sets for fluorescein. Images were analyzed using Comet IV software (Perceptive Instruments Ltd) with 200–600 comets measured per sample. A random sampling of 200 comets per condition was used for two-way analysis of variance (ANOVA) analysis (Prism software, GraphPad) of three biological replicates.

Xenograft assays

Male severe combined immunodeficiency (SCID) mice (4–6 weeks old) were obtained from a breeding colony maintained by the University of Michigan. Tumors were induced by subcutaneous injection of $1x10^6$ VCaP cells (10 mice per dose group) in 200 μL of Matrigel (BD Biosciences, Inc., San Jose, CA) above the right flank. Tumor growth was monitored by caliper measurement until the tumor size reached 100 mm^3 using the formula $0.56\ x\ L\ x\ W^2$. Groups were randomized and all mice were treated subcutaneously with control (DMSO) or with polyamide **1** as reported (3 times per week, 10 total injections). Tumor growth was followed weekly by caliper measurements. Animal husbandry and daily care and medical supervision was provided by the staff of the Unit for Laboratory Animal Medicine (ULAM) under the guidance of supervisors who are certified as Animal Technologists by the American Association for Laboratory Animal Science (AALAS) at the University of Michigan. Animals were monitored twice daily by both the research team and the veterinary staff. Health was monitored by weight (twice weekly), food and water intake, and general assessment of animal activity, panting, and fur condition. The experiments were performed in accordance with the guidelines on the care and use of animals set by the University Committee for the Use and Care of Animals (UCUCA) of the University of Michigan, and all procedures in this study were specifically approved by the UCUCA (Protocol Number 3848). In all cases, appropriate measures were taken to minimize discomfort to animals. All injections or surgical procedures were performed using sterile technique with efforts made to minimize trauma to the animals. When necessary, animals were anesthetized with a mixture of 1.75% isofluorane/air. Following injections animals were closely monitored and any that appeared moribund were immediately euthanized by administration of anesthesia, followed by inhalation of carbon dioxide until breathing ceased. Death was then ensured through cervical dislocation.

RNA-seq analysis

VCaP cells ($1x10^6$ cells) were plated in 20 cm cell culture dishes and allowed to adhere for 72 h in DMEM containing 10% FBS and 4 mM glutamine. Polyamide **1** or 0.1% DMSO vehicle were then added in fresh media and allowed to incubate for 96 h. Total RNA was collected by trizol extraction. Library building and sequencing were performed at the Caltech Millard and Muriel Jacobs Genetics and Genomics Laboratory. Sequenced reads were mapped against the human genome (hg19) with Tophat2 using Ensembl GRCh37 gene annotations [31]. Exon alignment was performed with htseq-count and differential expression was determined with DESeq2 [32, 33]. Genes with padj < 0.05 and $|\log_2(\text{fold change})| \geq 1$ were submitted for connectivity map analysis online at http://lincscloud.org.

Topoisomerase inhibition assay

Topoisomerase inhibition kits were purchased from Topogen (Port Orange, FL). For Top2 relaxation assays, 540 ng Top2α-p170 fragment (16 units) was added to 250 ng supercoiled pHOT1 DNA in assay buffer (0.05 M Tris-HCl (pH 8), 0.15 M NaCl, 10 mM MgCl2, 0.5 mM dithiothreitol) plus 2 mM ATP with or without test compounds in a total volume of 20 μL. The DMSO concentration was standardized to 1% for all samples except the no-DMSO solvent controls. Reactions were incubated at 37°C for 30 min and then quenched with 2 μL 10% sodium dodecyl sulfate solution. Samples were then extracted with chloroform: isoamyl alcohol 24:1, mixed with 2 μL 10x glycerol loading buffer and loaded onto 1% agarose gels in tris-acetic acid-EDTA (TAE) buffer with or without 0.5 μg/mL ethidium bromide (EtBr). Gels run without EtBr were post-stained with SYBR-Gold (Invitrogen).

For Top1 assays, 0.5 μL Top1 (5 units) was added to 250 ng supercoiled pHOT1 DNA in assay buffer (10 mM Tris-HCl (pH 7.5), 1 mM EDTA) plus 2 μL reaction buffer (10 mM Tris-HCl (pH 7.9), 1 mM EDTA, 0.15 M NaCl, 0.1% BSA, 0.1 mM spermidine, 5% glycerol) with or without test compounds in a total volume of 20 μL. The DMSO concentration was again standardized to 1% for all samples except the no-DMSO solvent controls. Reactions were incubated at 37°C for 30 min and then quenched with 4 μL stop buffer (0.125% bromphenol blue, 25% glycerol, 5% Sarkosyl). Samples were then loaded onto 1% agarose gels in tris-acetic acid-EDTA (TAE) buffer with or without 0.5 μg/mL ethidium bromide (EtBr). Gels run without EtBr were post-stained with SYBR-Gold.

Results

Nuclear uptake and cytotoxicity of Py-Im polyamide

To test the nuclear uptake potential of polyamide **1**, a FITC-labeled derivative was prepared (**1-FITC**) and incubated with VCaP cells prior to imaging by confocal microscopy (S1 Fig). Polyamide **1-FITC** signal was observed in the nucleus and also showed significant membrane binding. The overall level of uptake in VCaP cells was found to be qualitatively less than that in LNCaP cells [21]. Next, polyamide **1** was evaluated for antiproliferation effects in VCaP cells using the WST-1 assay under conditions similar to the gene expression experiment. After a 96 h incubation with polyamide, an IC_{50} value of 6.5 ± 0.3 μM was determined for polyamide **1** (Fig 2A). At 72 h, the IC_{50} value for polyamide **1** in VCaP cells was found to be over 30 μM (data not shown). For comparison, polyamide **1** has been found to have an IC_{50} of 7 ± 3 μM after 72 h incubation in LNCaP cells [19].

Reduction of DNA damage in VCaP cells upon treatment with Py-Im polyamide

The effect of polyamide **1** on the high level of extant DNA damage in VCaP cells was also investigated. After incubation with polyamide, VCaP cells were submitted to the neutral Comet assay, which allows visualization of double-strand breaks through single cell electrophoresis (Fig 2B). The percentage of DNA in the "tail" of the comets was then compared using two-way ANOVA statistical analysis (S4 Fig). A significant reduction in DNA damage ($p < 0.001$) was observed with polyamide **1** over the vehicle control.

ARE-targeted Py-Im polyamide downregulates AR-driven *TMPRSS2-ERG* expression

Next the effect of polyamide **1** on AR signaling in ERG-positive cells was examined. Dosage concentrations were chosen based on previous reports of polyamide gene expression effects in LNCaP [28, 34]. In VCaP cells, polyamide **1** was found to reduce the DHT-induced expression of the *TMPRSS2-ERG* fusion as well as other AR target genes, including *PSA* and *FKBP5* (Fig 2C). Corresponding decreased expression of ERG protein was confirmed by Western blot (Fig 2D). In the non-induced state, polyamide **1** was also found to reduce expression of several ERG influenced genes, including *PLAT* and *MYC* (S5 Fig).

Diminished growth in VCaP xenografts upon polyamide treatment

We next moved from cell culture studies to investigations of polyamide **1** in a VCaP mouse xenograft tumor model. Xenograft experiments were conducted in male SCID mice bearing subcutaneous VCaP cell xenografts. Treatments were started after tumor sizes in each group of mice reached ~100 mm^3 and were administered three times per week through subcutaneous

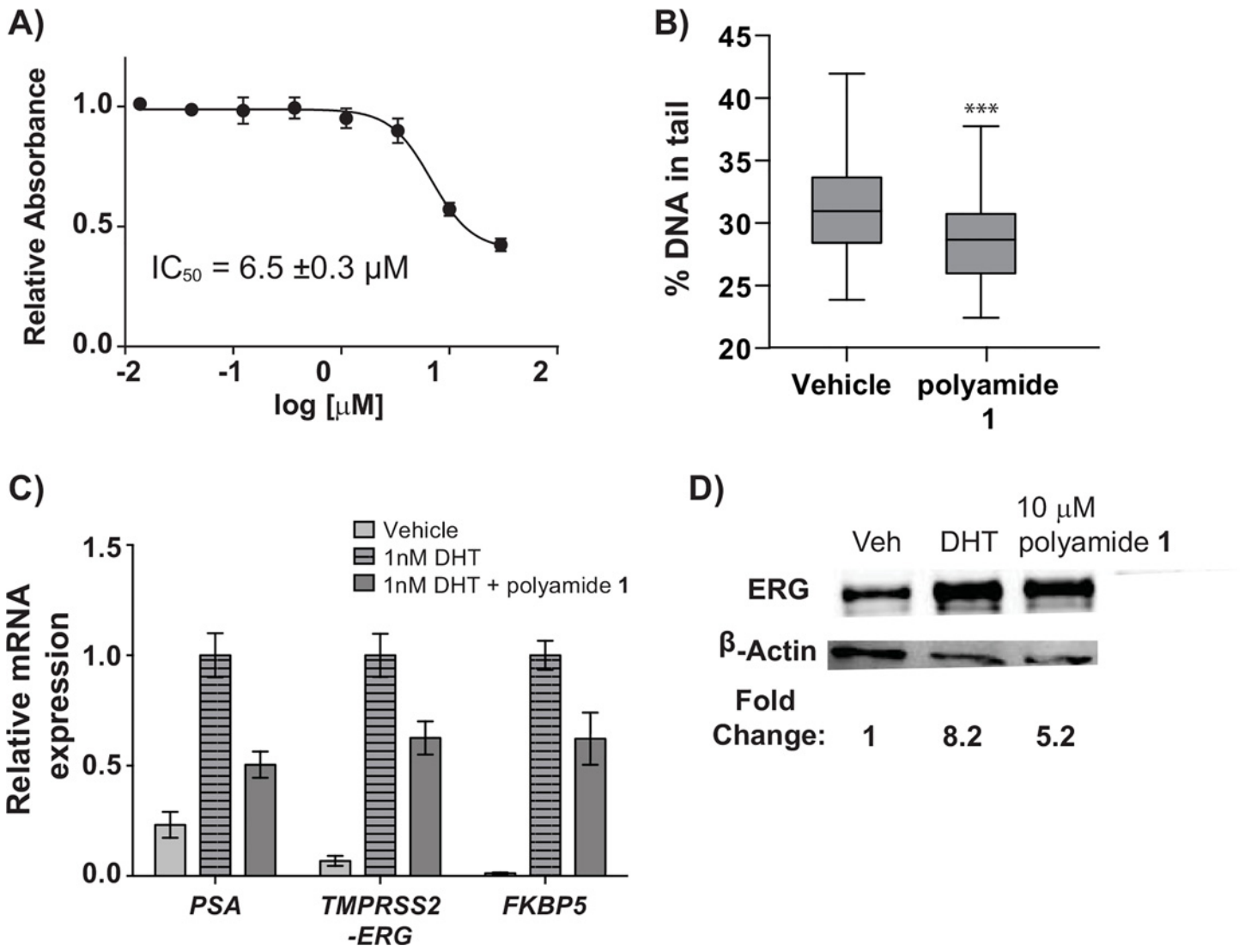

Fig 2. Cell culture characterization of polyamide 1 in VCaP cells. (A) Cytotoxicity of polyamide **1** in VCaP cells after 96 h incubation. (B) Quantification of 200 neutral comets from VCaP cells treated with 0.1% DMSO (vehicle) or 10 μM polyamide **1** for 72 h. Statistical significance was determined using two-way ANOVA analysis (Prism) where *** = $p < 0.001$ relative to vehicle. Boxes are bounded by the upper and lower quartile, while whiskers represent the 1st and 99th percentile. (C) Effect of 10 μM polyamide **1** on select androgen receptor regulated genes in VCaP cells under 1 nM DHT induction. (D) Change in ERG protein caused by 0.1% DMSO vehicle, 1 nM DHT alone, and cotreatment of 10 μM polyamide **1** with 1 nM DHT.

doi:10.1371/journal.pone.0143161.g002

injection in DMSO vehicle for three weeks for a total of 10 injections. Dose-dependent retardation of tumor growth was observed in mice treated with polyamide **1** (Fig 3). After 5 weeks of monitoring, tumors treated with vehicle grew to approximately 6-fold the initial volume of that group while tumors treated with polyamide **1** at 5.0 mg/kg grew to approximately 1.6-fold the initial volume of that cohort.

Genome wide expression analysis

RNA-seq analysis was performed after 96 hours of polyamide treatment in order to assess gene expression changes after prolonged exposure and to identify potential mechanisms of polyamide induced toxicity. Differential expression analysis using DESeq2 showed that of the genes

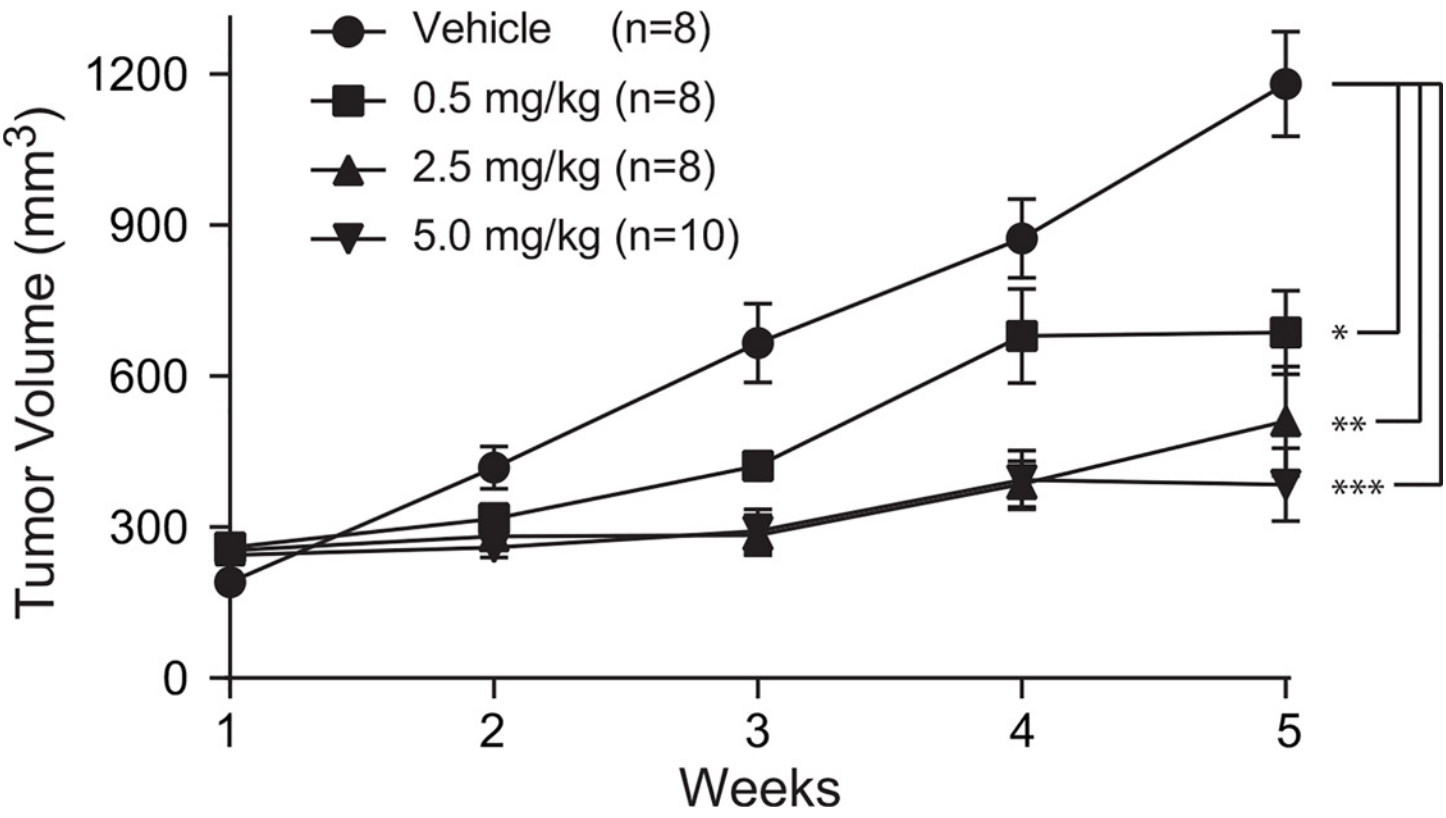

Fig 3. VCaP xenografts treated with polyamide 1 three times per week showed a dose dependent reduction in tumor growth. Tumor volume was determined by caliper measurements. Errors are SEM. * = p < 0.01, ** = p < 0.0005, *** = p < 0.0001.

doi:10.1371/journal.pone.0143161.g003

with padj < 0.05 and $|\log_2(\text{fold change})| \geq 1$, 342 were upregulated and 399 were downregulated upon polyamide treatment (Fig 4A). Connectivity map analysis of these genes returned several compounds known to be topoisomerase inhibitors (Fig 4B), suggesting that the polyamide may also be interfering with topoisomerase activity. Analysis of a previously published genome wide data set from LNCaP cells treated with polyamide **1** shows similar results (S6 Fig)[9].

Inhibition of topoisomerases 1 and 2

Topoisomerase inhibitors have been shown to attenuate AR signaling in multiple cell lines [35, 36]. Similar results are also seen in VCaP cells, where treatment with etoposide and camptothecin is able to reduce DHT induced expression of select AR regulated genes (S7 Fig). Based on the Connectivity map results, we examined the inhibitory effects of polyamide **1** against topoisomerase 1 and 2 *in vitro*. Topoisomerase 1 (Topo1) functions by relieving DNA supercoils generated by transcription and replication and is a therapeutic target in cancer [37]. To determine if polyamide **1** inhibits Topo1 mediated DNA cleavage, we titrated polyamide **1** with supercoiled pHOT1 plasmid and measured conversion to open circular plasmid or relaxation upon addition of purified Topo1. A reduction in DNA relaxation indicates polyamide **1** was able to attenuate Topo1 mediated cleavage of DNA (Fig 5A). To differentiate between open circular and relaxed DNA, samples were also run on an EtBr gel. Unlike camptothecin (CMT), which traps the Topo1 cleavage complex and generates nicked open circular DNA, treatment with polyamide **1** did not prevent DNA re-ligation. Topoisomerase II cleaves double stranded DNA in an ATP dependent manner and is essential for strand separation of tangled daughter

A)

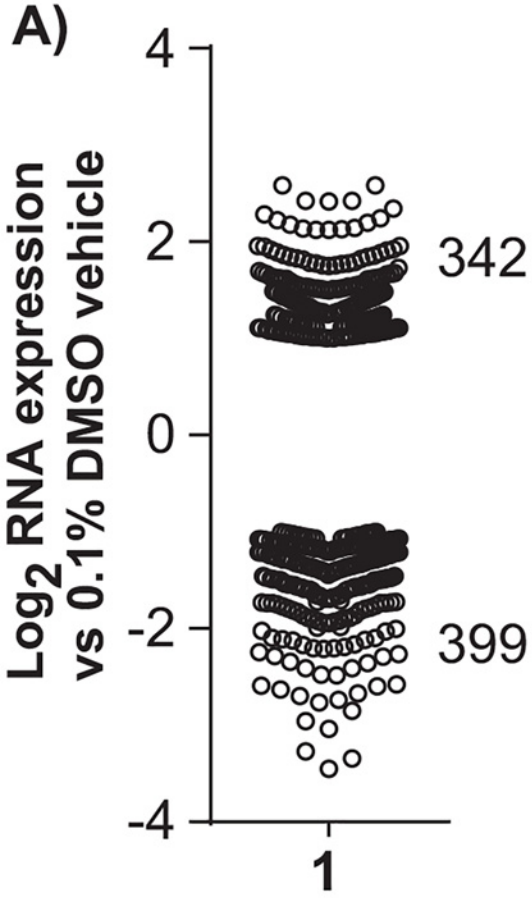

B)

	Compounds	Score
1	importazole	99.908
2	**SN-38**	99.781
3	pitavastatin	99.667
4	**amsacrine**	99.664
5	pyrvinium-pamoate	99.63
6	mitomycin-c	99.572
7	CD-437	99.303
8	**teniposide**	99.114
9	**camptothecin**	98.88
10	NSC-3852	98.559
11	**irinotecan**	98.552

Fig 4. Genome wide expression analysis of VCaP cells treated with 10 μM polyamide 1 for 96 h. (A) Scatter plot of gene expression changes in VCaP cells after polyamide treatment. (B) Connectivity map analysis of perturbagens that correlate with gene expression changes induced by polyamide **1**. Bolded compounds are topoisomerase inhibitors.

doi:10.1371/journal.pone.0143161.g004

chromosomes during replication. Like Topo1, Topo2 is targeted in cancer therapy [38]. Similar to results seen for Topo1, polyamide **1** was able to inhibit Topo2 cleavage of supercoiled pHOT1 plasmid in a concentration dependent manner (Fig 5B). Furthermore, samples were run with EtBr to allow unambiguous identification of linearized DNA, which allowed the identification of Topo2 cleavage complex (Topo2cc) formation (Fig 5B, lanes 5 and 6). The lack of Topo2cc formation in polyamide **1** treated samples as compared to linearized DNA and etoposide-treated samples is consistent with disruption of Topo2 binding.

Discussion

In this study, we evaluated the activity of an ARE targeted polyamide in VCaP human prostate cancer cells. Polyamide **1** has been previously shown to exhibit antitumor activity in cell culture and in xenografts of the androgen sensitive LNCaP cell line [19], but there are several important genotypic differences between these two cell lines. First, VCaP cells possess an amplified AR region, leading to higher levels of AR protein than LNCaP cells [30, 39, 40]. Additionally, VCaP cells belong to a subtype of prostate cancer that possesses the *TMPRSS2*:*ERG fusion*, resulting in the AR driven expression of *ERG* [23]. *ERG*, an oncogenic transcription factor, has been reported to increase double stranded DNA break formation in PrEC cells, while

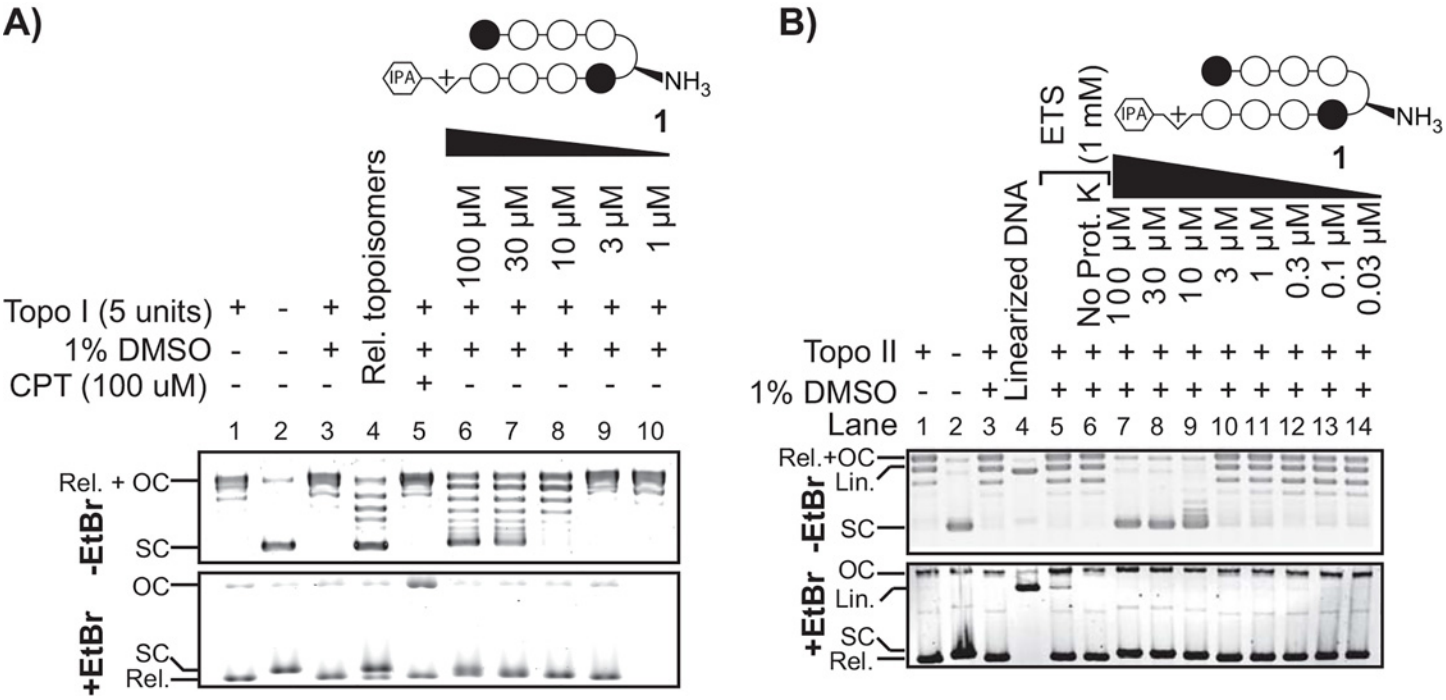

Fig 5. Inhibition of topoisomerase I and II by polyamide 1 in vitro. (A) Supercoiled DNA relaxation assay for topoisomerase I treated with increasing concentrations of polyamide **1**. Camptothecin (CPT) is used as a positive control. (B) Supercoiled DNA relaxation assay for topoisomerase IIα-p170 fragment. Etoposide (ETS) is used as a control. Rel, relaxed; OC, open circular; SC, supercoiled; Lin, linear; Rel. topoisomers, relaxed topoisomers; Prot. K, proteinase K.

doi:10.1371/journal.pone.0143161.g005

knockdown of *ERG* by siRNA in VCaP cells have been shown to decrease DNA breaks [41]. Studies have also shown that *ERG* overexpression increases cancer invasiveness and has been correlated to increased metastasis in the clinic [25, 26].

In VCaP cell culture experiments, polyamide **1** exhibited antiproliferative activity and attenuated the DHT induced expression of select AR driven genes including *TMPRSS2*:*ERG*. Furthermore, in this cell line with high genomic instability due to *ERG* overexpression, treatment with polyamide **1** repressed the high level of DNA fragmentation found in the basal state, which may be attributed to diminished ERG protein. *In vivo*, VCaP xenografts treated with polyamide **1** exhibited reduced growth in a dosage dependent manner, demonstrating its potential as an anticancer therapeutic.

To further examine the mechanism of action for polyamide **1**, we conducted gene expression analysis of VCaP cells after exposure to polyamide **1** in the same time frame as the cytotoxic experiment. Connectivity map analysis of gene expression signatures from treated VCaP cells indicated overlap with expression profiles of several topoisomerase inhibitors. *In vitro* assays for inhibition of both Topo1 and Topo2 confirmed that polyamide **1** is able to attenuate enzymatic activity of both enzymes. Similar results have been reported for other minor groove binders [42–47]. Furthermore, the lack of topoisomerase 2 cleavage complex formation in the inhibition assays suggests polyamide **1** functions by preventing protein-DNA interactions. This mechanism is in contrast to most drugs that target topoisomerases, which poison the enzymes. Drugs such as etoposide, doxorubicin, and camptothecin work by causing covalent adducts, which results in genotoxicity [48].

In addition to inhibition of Topo1 and Topo2, polyamide **1** has been reported to antagonize AR signaling, block RNA polymerase II elongation, and affect DNA replication by impeding

helicase processivity [19, 21, 49]. These effects may be related, as inhibition of Topo1 has been shown to lead to RNA polymerase II and DNA polymerase stalling [50], and treatment of prostate cancer cells with topoisomerase inhibitors has been shown to attenuate AR signaling [35, 36, 51, 52]. Taken together, these data suggest that by virtue of targeting DNA and DNA:protein interactions, polyamide **1** may exhibit antiproliferative effects on cancer cells through polypharmacological mechanisms without inducing genotoxic stress.

Supporting Information

S1 Fig. (A) Chemical structure of 1-FITC. (B) Nuclear localization of 1-FITC in VCaP cells are 24 h and 48 h incubation.
(PNG)

S2 Fig. Mass spectrometry data for Py-Im polyamides used. All polyamides were characterized using high resolution MALDI-TOF. Because this method leads to cleavage of fluorescein, FITC functionalized polyamides were also characterized by liquid chromatography coupled mass spectrometry (LCMS) equipped with a low resolution ionization spectrometer.
(PNG)

S3 Fig. Primer sequences for qPCR analysis. Sequences for mRNA analysis without a listed reference (*) were designed using qPrimerDepot (primerdepot.nci.nih.gov), and the single amplification products verified by agarose gel electrophoresis against the 1.1 kN NEB ladder.
(PNG)

S4 Fig. Report of two-way ANOVA analysis from Prism software (GraphPad) for Comet assays in VCaP cells.
(PNG)

S5 Fig. (A) Table of mRNA expression levels for AR-driven genes under DHT-induced conditions in response to 10 μM polyamide 1. VCaP cells were plated at 31k/cm^2, treated with medium containing 0.1% DMSO (with or without polyamide) and charcoal-treated FBS (CT-FBS) for 72 h followed by induction with 1 nM dihydrotestosterone (DHT) or vehicle for an additional 24 h. *—mRNA expression levels below threshold. (B) mRNA expression data for polyamides at 1 and 10 μM concentration. VCaP cells plated at 31k/cm^2 were treated with medium containing 0.1% DMSO vehicle (with or without polyamide) for 72h. mRNA levels were measured by qPCR, referenced to *GUSB*, and the polyamide effects compared to vehicle treated samples. Data shown are average of the fold changes (treated/untreated) for three or more biological replicates +/- standard error.
(PNG)

S6 Fig. Connectivity map analysis of perturbagens that correlate with gene expression changes induced by polyamide 1 in LNCaP cells. Bolded compounds are topoisomerase inhibitors.
(PNG)

S7 Fig. Effect of topoisomerase inhibitors on gene expression in VCaP cells. VCaP cells were plated at 31k/cm^2, incubated for 24 h, and then treated with medium containing 0.1% DMSO (with or without camptothecin or etoposide) and DHT for 16 h. mRNA levels were measured by qPCR, referenced to *GUSB*, and the effects compared to vehicle treated samples. Data shown are the average fold changes (treated/untreated) for three biological replicates +/- standard error.
(PNG)

Acknowledgments

Mass spectrometry analyses were performed in the Mass Spectrometry Laboratory of the Division of Chemistry and Chemical Engineering at the California Institute of Technology, imaging was performed at the Caltech Bioimaging Center in the Beckman Institute, and sequencing was performed at the Millard and Muriel Jacobs Genetics and Genomics Laboratory at California Institute of Technology.

Author Contributions

Conceived and designed the experiments: AEH TFM AAH AAK JWP SS KJP PBD. Performed the experiments: AEH TFM AAH AAK JWP SS. Analyzed the data: AEH TFM AAH AAK JWP SS KJP PBD. Contributed reagents/materials/analysis tools: AEH AAH JWP. Wrote the paper: AEH TFM AAH AAK JWP KJP PBD.

References

1. Kielkopf CL, Baird EE, Dervan PB, Rees DC. Structural basis for G.C recognition in the DNA minor groove. Nature structural biology. 1998; 5(2):104–9. PMID: 9461074
2. Kielkopf CL, White S, Szewczyk JW, Turner JM, Baird EE, Dervan PB, et al. A structural basis for recognition of A.T and T.A base pairs in the minor groove of B-DNA. Science. 1998; 282(5386):111–5. PMID: 9756473
3. Chenoweth DM, Dervan PB. Allosteric modulation of DNA by small molecules. Proc Natl Acad Sci U S A. 2009; 106(32):13175–9. doi: 10.1073/pnas.0906532106 PMID: 19666554
4. Chenoweth DM, Dervan PB. Structural Basis for Cyclic Py-Im Polyamide Allosteric Inhibition of Nuclear Receptor Binding. Journal of the American Chemical Society. 2010; 132(41):14521–9. doi: 10.1021/ja105068b PMID: 20812704
5. Best TP, Edelson BS, Nickols NG, Dervan PB. Nuclear localization of pyrrole-imidazole polyamide-fluorescein conjugates in cell culture. Proc Natl Acad Sci U S A. 2003; 100(21):12063–8. PMID: 14519850
6. Edelson BS, Best TP, Olenyuk B, Nickols NG, Doss RM, Foister S, et al. Influence of structural variation on nuclear localization of DNA-binding polyamide-fluorophore conjugates. Nucleic acids research. 2004; 32(9):2802–18. PMID: 15155849
7. Nickols NG, Jacobs CS, Farkas ME, Dervan PB. Improved nuclear localization of DNA-binding polyamides. Nucleic acids research. 2007; 35(2):363–70. PMID: 17175539
8. Muzikar KA, Nickols NG, Dervan PB. Repression of DNA-binding dependent glucocorticoid receptor-mediated gene expression. Proc Natl Acad Sci U S A. 2009; 106(39):16598–603. doi: 10.1073/pnas.0909192106 PMID: 19805343
9. Nickols NG, Dervan PB. Suppression of androgen receptor-mediated gene expression by a sequence-specific DNA-binding polyamide. Proc Natl Acad Sci U S A. 2007; 104(25):10418–23. PMID: 17566103
10. Nickols NG, Jacobs CS, Farkas ME, Dervan PB. Modulating hypoxia-inducible transcription by disrupting the HIF-1-DNA interface. ACS Chem Biol. 2007; 2(8):561–71. PMID: 17708671
11. Olenyuk BZ, Zhang GJ, Klco JM, Nickols NG, Kaelin WG Jr, Dervan PB. Inhibition of vascular endothelial growth factor with a sequence-specific hypoxia response element antagonist. Proc Natl Acad Sci U S A. 2004; 101(48):16768–73. PMID: 15556999
12. Muzikar KA, Meier JL, Gubler DA, Raskatov JA, Dervan PB. Expanding the repertoire of natural product-inspired ring pairs for molecular recognition of DNA. Organic letters. 2011; 13(20):5612–5. doi: 10.1021/ol202285y PMID: 21957930
13. Raskatov JA, Meier JL, Puckett JW, Yang F, Ramakrishnan P, Dervan PB. Modulation of NF-kappaB-dependent gene transcription using programmable DNA minor groove binders. Proc Natl Acad Sci U S A. 2012; 109(4):1023–8. doi: 10.1073/pnas.1118506109 PMID: 22203967
14. Chen CD, Welsbie DS, Tran C, Baek SH, Chen R, Vessella R, et al. Molecular determinants of resistance to antiandrogen therapy. Nat Med. 2004; 10(1):33–9. PMID: 14702632
15. Tsai MJ, O'Malley BW. Molecular mechanisms of action of steroid/thyroid receptor superfamily members. Annual review of biochemistry. 1994; 63:451–86. PMID: 7979245
16. Taylor BS, Schultz N, Hieronymus H, Gopalan A, Xiao Y, Carver BS, et al. Integrative genomic profiling of human prostate cancer. Cancer cell. 2010; 18(1):11–22. doi: 10.1016/j.ccr.2010.05.026 PMID: 20579941

17. Tyagi RK, Lavrovsky Y, Ahn SC, Song CS, Chatterjee B, Roy AK. Dynamics of intracellular movement and nucleocytoplasmic recycling of the ligand-activated androgen receptor in living cells. Molecular endocrinology. 2000; 14(8):1162–74. PMID: 10935541

18. Roche PJ, Hoare SA, Parker MG. A consensus DNA-binding site for the androgen receptor. Molecular endocrinology. 1992; 6(12):2229–35. PMID: 1491700

19. Yang F, Nickols NG, Li BC, Marinov GK, Said JW, Dervan PB. Antitumor activity of a pyrrole-imidazole polyamide. Proc Natl Acad Sci U S A. 2013; 110(5):1863–8. doi: 10.1073/pnas.1222035110 PMID: 23319609

20. Synold TW, Xi B, Wu J, Yen Y, Li BC, Yang F, et al. Single-dose pharmacokinetic and toxicity analysis of pyrrole-imidazole polyamides in mice. Cancer chemotherapy and pharmacology. 2012; 70(4):617–25. PMID: 22907527

21. Yang F, Nickols NG, Li BC, Szablowski JO, Hamilton SR, Meier JL, et al. Animal toxicity of hairpin pyrrole-imidazole polyamides varies with the turn unit. Journal of medicinal chemistry. 2013; 56(18):7449–57. doi: 10.1021/jm401100s PMID: 24015881

22. Perlmutter MA, Lepor H. Androgen deprivation therapy in the treatment of advanced prostate cancer. Reviews in urology. 2007; 9 Suppl 1:S3–8. PMID: 17387371

23. Tomlins SA, Rhodes DR, Perner S, Dhanasekaran SM, Mehra R, Sun XW, et al. Recurrent fusion of TMPRSS2 and ETS transcription factor genes in prostate cancer. Science. 2005; 310(5748):644–8. PMID: 16254181

24. Perner S, Demichelis F, Beroukhim R, Schmidt FH, Mosquera JM, Setlur S, et al. TMPRSS2:ERG fusion-associated deletions provide insight into the heterogeneity of prostate cancer. Cancer research. 2006; 66(17):8337–41. PMID: 16951139

25. Demichelis F, Fall K, Perner S, Andren O, Schmidt F, Setlur SR, et al. TMPRSS2:ERG gene fusion associated with lethal prostate cancer in a watchful waiting cohort. Oncogene. 2007; 26(31):4596–9. PMID: 17237811

26. Tomlins SA, Laxman B, Varambally S, Cao X, Yu J, Helgeson BE, et al. Role of the TMPRSS2-ERG gene fusion in prostate cancer. Neoplasia. 2008; 10(2):177–88. PMID: 18283340

27. Puckett JW, Green JT, Dervan PB. Microwave assisted synthesis of Py-Im polyamides. Organic letters. 2012; 14(11):2774–7. doi: 10.1021/ol3010003 PMID: 22578091

28. Dose C, Farkas ME, Chenoweth DM, Dervan PB. Next generation hairpin polyamides with (R)-3,4-diaminobutyric acid turn unit. Journal of the American Chemical Society. 2008; 130(21):6859–66. doi: 10.1021/ja800888d PMID: 18459783

29. Li BC, Montgomery DC, Puckett JW, Dervan PB. Synthesis of cyclic Py-Im polyamide libraries. The Journal of organic chemistry. 2013; 78(1):124–33. doi: 10.1021/jo302053v PMID: 23106218

30. Korenchuk S, Lehr JE, L MC, Lee YG, Whitney S, Vessella R, et al. VCaP, a cell-based model system of human prostate cancer. In vivo. 2001; 15(2):163–8. PMID: 11317522

31. Trapnell C, Roberts A, Goff L, Pertea G, Kim D, Kelley DR, et al. Differential gene and transcript expression analysis of RNA-seq experiments with TopHat and Cufflinks. Nature protocols. 2012; 7(3):562–78. doi: 10.1038/nprot.2012.016 PMID: 22383036

32. Anders S, Pyl PT, Huber W. HTSeq—a Python framework to work with high-throughput sequencing data. Bioinformatics. 2015; 31(2):166–9. doi: 10.1093/bioinformatics/btu638 PMID: 25260700

33. Love MI, Huber W, Anders S. Moderated estimation of fold change and dispersion for RNA-seq data with DESeq2. Genome biology. 2014; 15(12):550. PMID: 25516281

34. Chenoweth DM, Harki DA, Phillips JW, Dose C, Dervan PB. Cyclic Pyrrole-Imidazole Polyamides Targeted to the Androgen Response Element. Journal of the American Chemical Society. 2009; 131(20):7182–8. doi: 10.1021/ja901309z PMID: 19413319

35. Haffner MC, Aryee MJ, Toubaji A, Esopi DM, Albadine R, Gurel B, et al. Androgen-induced TOP2B-mediated double-strand breaks and prostate cancer gene rearrangements. Nature genetics. 2010; 42(8):668–75. doi: 10.1038/ng.613 PMID: 20601956

36. Li H, Xie N, Gleave ME, Dong X. Catalytic inhibitors of DNA topoisomerase II suppress the androgen receptor signaling and prostate cancer progression. Oncotarget. 2015; 6(24):20474–84. PMID: 26009876

37. Pommier Y. Topoisomerase I inhibitors: camptothecins and beyond. Nature reviews Cancer. 2006; 6(10):789–802. PMID: 16990856

38. Nitiss JL. Targeting DNA topoisomerase II in cancer chemotherapy. Nature reviews Cancer. 2009; 9(5):338–50. doi: 10.1038/nrc2607 PMID: 19377506

39. Makkonen H, Kauhanen M, Jaaskelainen T, Palvimo JJ. Androgen receptor amplification is reflected in the transcriptional responses of Vertebral-Cancer of the Prostate cells. Molecular and cellular endocrinology. 2011; 331(1):57–65. doi: 10.1016/j.mce.2010.08.008 PMID: 20728506

40. Liu W, Xie CC, Zhu Y, Li T, Sun J, Cheng Y, et al. Homozygous deletions and recurrent amplifications implicate new genes involved in prostate cancer. Neoplasia. 2008; 10(8):897–907. PMID: 18670647

41. Brenner JC, Ateeq B, Li Y, Yocum AK, Cao Q, Asangani IA, et al. Mechanistic rationale for inhibition of poly(ADP-ribose) polymerase in ETS gene fusion-positive prostate cancer. Cancer cell. 2011; 19 (5):664–78. doi: 10.1016/j.ccr.2011.04.010 PMID: 21575865

42. Kim SO, Sakchaisri K, Thimmegowda NR, Soung NK, Jang JH, Kim YS, et al. STK295900, a dual inhibitor of topoisomerase 1 and 2, induces G(2) arrest in the absence of DNA damage. PloS one. 2013; 8 (1):e53908. doi: 10.1371/journal.pone.0053908 PMID: 23349762

43. Beerman TA, McHugh MM, Sigmund R, Lown JW, Rao KE, Bathini Y. Effects of analogs of the DNA minor groove binder Hoechst 33258 on topoisomerase II and I mediated activities. Biochimica et biophysica acta. 1992; 1131(1):53–61. PMID: 1374646

44. Beerman TA, Woynarowski JM, Sigmund RD, Gawron LS, Rao KE, Lown JW. Netropsin and bisnetropsin analogs as inhibitors of the catalytic activity of mammalian DNA topoisomerase II and topoisomerase cleavable complexes. Biochimica et biophysica acta. 1991; 1090(1):52–60. PMID: 1653020

45. McHugh MM, Sigmund RD, Beerman TA. Effects of minor groove binding drugs on camptothecin-induced DNA lesions in L1210 nuclei. Biochemical pharmacology. 1990; 39(4):707–14. PMID: 1689578

46. McHugh MM, Woynarowski JM, Sigmund RD, Beerman TA. Effect of minor groove binding drugs on mammalian topoisomerase I activity. Biochemical pharmacology. 1989; 38(14):2323–8. PMID: 2473754

47. Woynarowski JM, Sigmund RD, Beerman TA. DNA minor groove binding agents interfere with topoisomerase II mediated lesions induced by epipodophyllotoxin derivative VM-26 and acridine derivative m-AMSA in nuclei from L1210 cells. Biochemistry. 1989; 28(9):3850–5. PMID: 2473776

48. Pommier Y, Leo E, Zhang H, Marchand C. DNA Topoisomerases and Their Poisoning by Anticancer and Antibacterial Drugs. Chemistry & Biology. 2010; 17(5):421–33. doi: 10.1016/j.chembiol.2010.04.012 PMID: 20534341

49. Martinez TF, Phillips JW, Karanja KK, Polaczek P, Wang CM, Li BC, et al. Replication stress by Py-Im polyamides induces a non-canonical ATR-dependent checkpoint response. Nucleic Acids Res. 2014; 42(18):11546–59. doi: 10.1093/nar/gku866 PMID: 25249630

50. Tuduri S, Crabbe L, Conti C, Tourriere H, Holtgreve-Grez H, Jauch A, et al. Topoisomerase I suppresses genomic instability by preventing interference between replication and transcription. Nature cell biology. 2009; 11(11):1315–24. doi: 10.1038/ncb1984 PMID: 19838172

51. Liu S, Yamauchi H. Etoposide induces growth arrest and disrupts androgen receptor signaling in prostate cancer cells. Oncology reports. 2010; 23(1):165–70. PMID: 19956877

52. Liu S, Yuan Y, Okumura Y, Shinkai N, Yamauchi H. Camptothecin disrupts androgen receptor signaling and suppresses prostate cancer cell growth. Biochemical and biophysical research communications. 2010; 394(2):297–302. doi: 10.1016/j.bbrc.2010.02.164 PMID: 20206136